HHS Public Access

Author manuscript

Adv Sci (Weinh). Author manuscript; available in PMC 2015 September 14.

Published in final edited form as:

Adv Sci (Weinh). 2015 August ; 2(8): . doi:10.1002/advs.201500025.

Massive Bioaccumulation and Self-Assembly of Phenazine Compounds in Live Cells

Dr. Kyoung Ah Min[a], **Dr. Walajapet G. Rajeswaran**[b], **Rudolf Oldenbourg**[c] **[Prof.]**, **Grant Harris**[c], **Dr. Rahul K. Keswani**[a], **Mason Chiang**[a], **Phillip Rzeczycki**[a], **Arjang Talattof**[a], **Mahwish Hafeez**[a], **Richard W. Horobin**[d] **[Prof.]**, **Dr. Scott D. Larsen**[b] **[Prof.]**, **Dr. Kathleen A. Stringer**[e] **[Prof.]**, and **Dr. Gus R. Rosania**[a] **[Prof.]**

[a]Department of Pharmaceutical Sciences, University of Michigan College of Pharmacy, 428 Church St, Ann Arbor, MI 48109

[b]Department of Medicinal Chemistry, University of Michigan College of Pharmacy, 428 Church St, Ann Arbor, MI 48109, Ann Arbor, MI 48109

[c]Marine Biological Laboratories, Woods Hole, MA 02543

[d]School of Life Sciences, The University of Glasgow, University Avenue, Glasgow G12 8QQ, Scotland UK

[e]Department of Clinical, Social and Administrative Sciences, University of Michigan College of Pharmacy, Ann Arbor, MI 48109

Abstract

Clofazimine is an orally administered, FDA-approved drug that massively bioaccumulates in macrophages, forming membrane-bound intracellular structures possessing nanoscale supramolecular features. Here, a library of phenazine compounds derived from clofazimine was synthesized and tested for their ability to accumulate and form ordered molecular aggregates inside cells. Regardless of chemical structure or physicochemical properties, bioaccumulation was consistently greater in macrophages than in epithelial cells. Microscopically, some self-assembled structures exhibited a pronounced, diattenuation anisotropy signal, evident by the differential absorption of linearly polarized light, at the peak absorbance wavelength of the phenazine core. The measured anisotropy was well above the background anisotropy of endogenous cellular components, reflecting the self-assembly of condensed, insoluble complexes of ordered phenazine molecules. Chemical variations introduced at the R-imino position of the phenazine core led to idiosyncratic effects on the compounds‘ bioaccumulation behavior, as well as on the morphology and organization of the resulting intracellular structures. Beyond clofazimine, these results demonstrate how the self-assembly of membrane-permeant, orally-bioavailable small molecule building blocks can endow cells with unnatural structural elements possessing chemical, physical and functional characteristics unlike those of other natural cellular components.

Correspondence to: Gus R. Rosania.

Fax: 734-615-6162, grosania@umich.edu.

Supporting Information

Supporting Information is available from the Wiley Online Library or from the author.

Keywords

Medicinal chemistry; clofazimine; imaging; aggregation; chromophores; biocrystals; polarization

1. Introduction

In mammals, macrophages orchestrate many key physiological functions, including wound healing and regeneration, clearance of apoptotic and necrotic cells, recognition of foreign antigens, defense against invading pathogens and mounting of protective immune responses.[1] In addition, macrophages play a physiological role in the disposition of lipophilic, poorly soluble small molecule chemical agents. In the liver, for example, Kupffer cells sequester lipids, cholesterol, fat soluble vitamins, xenobiotics and drugs.[2] Perhaps it is not too surprising that clofazimine, an old but highly effective antibiotic that is included in the World Health Organization's list of essential medications and part of the standard treatment of leprosy[3], has been found to massively bioaccumulate in macrophages.[4] In these cells, clofazimine forms crystal-like drug inclusions (CLDIs): highly organized, insoluble molecular complexes that are predominantly found in membrane-bound compartments within the cytoplasm.[4] Although drug crystal formation has generally been regarded as an unwanted side effect, clofazimine is a well-tolerated, clinically useful drug. Thus, in the case of clofazimine, CLDIs may function as a biocompatible, intracellular drug depot mechanism. More generally, CLDI formation could be exploited as a means to target drugs to macrophages in living organisms, and to endow these cells with unnatural structural and functional elements for diagnostic or therapeutic purposes.

Related to clofazimine, Neutral Red is a phenazine compound that undergoes accumulation in lysosomes,[5] while Janus Green B is another phenazine compound that undergoes electrical potential dependent accumulation in mitochondria.[6] However, neither of these compounds exhibits the massive intracellular bioaccumulation or intracellular self-assembly properties that are characteristic of clofazimine. Furthermore, because of differences in membrane partitioning, the transport mechanisms mediating the cellular uptake and intracellular distribution of clofazimine may be different from that of less lipophilic, more soluble phenazine derivatives[8]. Therefore, to explore whether other phenazine compounds could provide a good a starting point for developing new kinds of self-assembling intracellular elements for drug delivery and bioimaging applications, we decided to examine the impact of variations in lipophilicity and chemical structure on the intracellular uptake and trafficking of phenazine compounds. For this purpose, we synthesized a small, focused library of phenazine derivatives of clofazimine, and assayed their bioaccumulation and self-assembly properties in RAW 264.7 macrophages and Madin-Darby Canine Kidney (MDCK) epithelial cells.

Because phenazines are chromophores with a broad absorbance peak in the range of visible wavelengths, the interaction of the phenazine ring with monochromic, polarized light could be useful to specifically probe the intracellular accumulation, distribution and molecular organization of the phenazine compounds. Accordingly, a quantitative polarization microscope (LC-PolScope)[9] was adapted to assay the formation of condensed, ordered

molecular aggregates of the compounds in live cells. With this instrument, we measured the manner in which the intracellular inclusions differentially influenced the transmittance of polarized light –an optical property known as diattenuation anisotropy[10]. By relating the extent of bioaccumulation to the measured optical properties of the intracellular inclusions formed by different phenazine derivatives, we determined that certain chemical modifications at the R-imino group promoted the self-assembly of phenazines, specifically in macrophages. The influence of these variations on bioaccumulation and structure formation seemed highly idiosyncratic. However, all compounds tended to preferentially accumulate in macrophages relative to epithelial cells, regardless of their chemical structure or physicochemical properties.

2. Results and Discussion

First, we synthesized a focused library of clofazimine derivatives (Scheme 1), by replacing the chlorophenyl moieties of clofazimine with different aromatic substituents (Figure 1a and Table S1, Compounds A to G). When these compounds were incubated with cells, they exhibited similar or decreased intracellular staining relative to clofazimine, irrespective of their higher or lower lipophilicity relative to clofazimine (Figure 1a‘; Table S2). Small changes in the chemical structure of clofazimine were associated with visibly different cellular staining pattern in macrophages. In this first series of phenazine compounds (Compounds A – G), the chlorophenyl moiety of clofazimine was replaced with various other closely related substituents, yet most of these substituents (Compounds A through F) led to decreased cellular staining in relation to clofazimine. Only the replacement of chlorines with hydroxyls led to a staining pattern similar to that of clofazimine (Compound G).

For comparison, we synthesized a second, focused series of derivatives, in which the isopropyl group at the R-imino position of clofazimine was replaced with different achiral substitutents (Figure 1b and Table S3, Compounds H to Q). Compared to clofazimine, replacing the isopropyl group with other functional groups at the R-imino position generally led to similar or greater staining of macrophages (Figure 1b‘ and Table S4; Compounds H to Q). Three derivatives yielded cellular staining patterns comparable in morphology and intensity to those of clofazimine (Compounds H, I, and M) while two derivatives yielded more prominent staining patterns (Compounds P and Q). The most intense staining was associated with the formation of condensed cytoplasmic inclusions, either amorphous or crystal-like in morphology (Figure 1b‘ and Table S4; Compounds P and Q).

To assess the extent to which specific interactions with chiral components present in cells (or the cell culture medium) affected the bioaccumulation and self-organization behavior of the compounds, we proceeded to synthesize and screen a third, focused series of phenazine derivatives, which incorporated a stereochemical center at the R-imino position (Figure 1c and Table S5, Compounds R to W). As observed in the second series of achiral R-imino phenazines, small variations in the chemical structure and physicochemical properties of these chiral R-imino phenazine compounds led to pronounced differences in cellular staining (Figure 1c‘ and Table S6). Three of the six chiral R-imino derivatives exhibited prominent cellular staining, associated with the formation of yellow, orange, red or brown cytoplasmic

inclusions (Figure 1c‘ and Table S6; Compounds U, V and W). In control experiments, untreated cells showed no visible yellow or brown staining when viewed using the same optical set up under transmitted, brightfield illumination (Figure 1d, Control). Furthermore, staining was also not observed when cells were fixed prior to incubation with the compounds (Table S6), indicating that the observed staining patterns reflected underlying differences in physiological, small molecule transport mechanisms present in live cells. Because all phenazine compounds exhibited similar absorbance spectra under different conditions (Figure 2a and b), the variations in cellular staining patterns most likely reflected differences in the accumulation and distribution of the compounds in the cells, independently from the compounds’ optical properties.

Next, we proceeded to characterize the optical properties of the inclusions using a quantitative, polarization microscope[9] to perform diattenuation anisotropy measurements on cells incubated with the different compounds[10]. By transmitting linearly polarized, monochromatic light of wavelengths near the absorbance maxima of the phenazine molecules, the diattenuation anisotropy signal can be used to detect and quantify the presence of ordered aggregates of phenazine molecules in live cells. For isotropic, disordered intracellular inclusions, polarized light is expected to be transmitted in the same manner irrespective of the orientation of the polarization vector, resulting in diattenuation anisotropy close to 0. For ordered intracellular inclusions of phenazine molecules (as occurs when molecules are aligned with each other), the diattenuation anisotropy should increase, as the ordered molecular aggregates will preferentially transmit light that is polarized in a particular direction. Accordingly, by comparing the diattenuation anisotropy image maps for treated and untreated control cells, we observed clear diattenuation anisotropy signals in association with dense inclusions formed specifically by phenazine compounds (see compounds P, U, V and W in Figure 3). Interestingly, compounds U, V and W exhibited optically anisotropic inclusions only in macrophages, whereas compound P formed optically anisotropic inclusions in both macrophages (Figure 3a) and epithelial cells (Figure 3b). By visual inspection, we observed significant variations in the molecular organization of the inclusions formed by different compounds: Some compounds formed monolithic aggregates comprised of a single domain with uniform orientation (Compound P; Figure 3a and b), while other compounds formed complex aggregates comprised of segregated domains with subdomains organized in different directions (Compounds U, V, W; Figure 3a).

We quantitatively confirmed that compounds P and Q showed higher diattenuation anisotropy in both macrophages and epithelial cells than seen with clofazimine (Figure 4a). Notably, chiral compounds U, V, and W exhibited even higher anisotropy as compared to clofazimine, but only in macrophages (Figure 4a). The measured diattenuation anisotropy signals for all chiral compounds were well above the background, diattenuation anisotropy signal of untreated cells (Figure 4a). On average, the anisotropy diattenuation ratio measured at a wavelength of 546 nm relative to 623 nm did not reveal significant wavelength-dependent differences in diattenuation anisotropy(Figure 4b), although some compounds exhibited higher variability in the measured diattenuation anisotropy ratios in macrophages than in epithelial cells (Figure 4; Compounds V and W).

In relation to the compounds‘ chemical structures, the self-assembly and resulting optical properties of intracellular structures formed by phenazine compounds appeared to be highly idiosyncratic: only one pair of enantiomers (Figure 3 and 4a, Compounds T and U) exhibited enantioselective differences in their optical anisotropy signal, and this was observed only in macrophages. Compunds V and W did not show enantioselective differences in diattenuation anisotropy (Figure 5a, b). The other pair of enantiomers (Compounds R and S) did not yield a measurable, diattenuation anisotropy signal in either macrophages or epithelial cells. Furthermore, Compound P, an achiral phenazine compound, formed inclusions with strong diattenuation anisotropy signals in both macrophages and epithelial cells (Figure 3 and 4), indicating that the formation of ordered, R-imino phenazine aggregates can occur regardless of stereochemistry.

To confirm the intracellular localization of the inclusions, we took advantage of the fluorescence properties of the phenazine compounds P, T and U. Following intracellular accumulation, these compounds exhibited strong fluorescence excitation and emission signals that were visible through the standard TRITC channel of a fluorescence, confocal microscope. Accordingly, we acquired confocal optical sections through cells incubated with these compounds to confirm that the inclusions were intracellularly localized (Figure 5). For counterstaining, cells were also incubated with an orthogonally fluorescent nuclear marker (Hoechst 33342), as well as an orthogonally fluorescent, plasma membrane-specific marker (FM-143). FM-143 yielded a green, plasma membrane signal in the FITC channel of the microscope, while Hoechst 33342 yielded a blue, nuclear signal in the DAPI channel. In both macrophages and epithelial cells, optical sections through the cells clearly revealed that Compounds P, T and U (red signals) were localized at the periphery of the cell nuclei (blue signal) and within the confines of the cells‘ plasma membrane (green signal) (Figure 5).

To establish the extent to which the differences in staining and self-assembly of phenazine compounds may be due to cell type-dependent differences in bioaccumulation, the total amount of compounds presentin macrophages (Figure 6a) and epithelial cells (Figure 6b) following an incubation period was measured and normalized by the number of cells. Overall, phenazine compounds tended to accumulate more in macrophages than in epithelial cells, regardless of ordered aggregate formation (Figure 6c). Nevertheless, compounds that exhibited the greatest accumulation in macrophages (Figure 6c and d) also yielded the most ordered inclusions (Compounds P, Q, U, V, and W). To confirm the cell type-dependence of the bioaccumulation and intracellular self-assembly properties of the phenazine compounds, principal component analysis (PCA) was performed on the cumulative bioaccumulation and diattenuation anisotropy data (Figure 7). Because the first two components of the resulting PCA plots captured >97% of the variation in the measured properties of the compounds in macrophages and epithelial cells (Figure 7), the PCA plot indicates that most of the observed variation was associated with cell type specific differences in bioaccumulation and diattenuation anisotropy, without a clear association with chirality, chemical structure or the lipophilicity of the compounds.

Lastly, we tested whether the bioaccumulation of the compounds was related to the precipitation of the compounds in cell culture media, or to their solubility. In serum containing media, solutions of clofazimine and the other phenazine compounds were stably

solubilized at the concentrations that were added to the cells, so the formation of extracellular precipitates is an unlikely explanation for the measured differences in bioaccumulation in either macrophages (Figure 8a) or epithelial cells (Figure 8b). Only one of the phenazine analogs (Compound J) was not completely solubilized under these conditions. In the absence of serum (Figure 8c and d), the phenazine compounds exhibited significant variation in their solubility with some of the compounds precipitating in the media. However, the solubility of the compounds did not show a correlation with the measured bioaccumulation in macrophages (Figure 8c) or epithelial cells (Figure 8d).

Considering the biological mechanisms that may account for the observed variations in bioaccumulation properties of phenazine compounds, clofazimine and other small molecule drugs can be subject to chemical transformation by metabolic enzymes. Furthermore, small organic molecules can also be substrates of active transport mechanisms. These metabolic and active transport mechanisms are differentially expressed in macrophages and epithelial cells, and they are highly specific and sensitive to the presence of different functional groups on the compounds.

3. Conclusion

To conclude, our results demonstrate that, in addition to clofazimine, other membrane-permeant small molecule phenazine compounds can bioaccumulate and self-assemble in macrophages, to a greater extent than in epithelial cells. Our results also demonstrate the use of monochromatic polarized light to measure diattenuation for monitoring the formation of ordered, insoluble complexes, which can be useful for assaying intracellular self-assembly of phenazine compounds. This is an advantage of this approach compared to other types of optical techniques that have been developed to detect the presence of insoluble drug complexes inside cells.[16] Indeed, with the quantitative polarization microscope, the presence of ordered molecular aggregates accompanying bioaccumulation of phenazine compounds was readily measurable and analyzable. Independently, we confirmed the bioaccumulation of the molecules by chemical analysis and the intracellular localization of the inclusions was confirmed with confocal microscopy by taking advantage of the compounds' fluorescence signals.

Similar to other structure-property relationship studies, our results demonstrate how the molecular organization of self-assembling intracellular elements can be analyzed in relation to specific chemical features of the individual, small molecule building blocks. Based on staining patterns, the uptake of clofazimine was inhibited by replacing its chlorophenyl group with different aromatic functionalities. Notably, modification of the R-imino group did not suppress intracellular inclusion formation. Instead, several R-imino phenazine derivatives exhibited greater bioaccumulation than clofazimine, forming highly condensed cytoplasmic inclusions, which exhibited strong diattenuation anisotropy signals. In addition, biological factors affecting the preferential bioaccumulation of phenazine molecules in macrophages exerted the most dominant effect on self-organization and intracellular inclusion formation, independently of the lipophilicity, solubility, and chirality of the molecules.

The condensation and phase separation of phenazine compounds into insoluble aggregates expecially influences the bioaccumulation and retention of these compounds inside macrophages. In this regard, it is important to note that the measured concentration of phenazine compounds inside cells is far greater than one would expect from a nonspecific partitioning or a specific binding mechanism. For all the compounds that bioaccumulated inside cells, the measured numbers of phenazine molecules per cell (>0.03 ± 0.01 picomoles) exceeded the amounts of the most concentrated, endogenous biomolecules and metabolites (e.g. ATP[11] or glutathione[12]). Only potassium and water are expected to be present in greater amounts.[13] Considering the possibility that bioaccumulation may reflect the partitioning of the molecules in membranes, there are in the order of 15 picograms of total lipids per leukocyte.[14] This corresponds to 0.03 picomoles of total lipids per cell (calculated based on 500 g/mol of phospholipid). Interestingly, such intracellular precipitation behavior has been reported for other kinds of drugs.[15] In fact, the size, faceted shapes, and overall morphology of these inclusions are inconsistent with the typical size, shapes and morphology of natural organelles[16] and do not resemble the typical staining patterns of mitochondria [17] or other cellular components stained with fluorescent probes.[18] Therefore, one can infer that in addition to cell type-specific differences in bioaccumulation, the propensity of poorly soluble phenazine molecules to aggregate into insoluble molecular complexes and phase separate from other cellular components also exerts an important influence on their intracellular disposition properties.

4. Experimental Section

Materials for chemical synthesis

The starting materials, reagents and solvents for the synthesis were purchased from Sigma Aldrich, Fisher Scientific Acros, Oakwood Products or Chem-Impex and used as such without purification. Biotage® Initiator Classic, single-mode Microwave Synthesizer was used for Microwave Syntheses. Compounds were purified by either Column Chromatography using Silicycle's SiliaFlash® P60 (220–240 mesh) under positive house nitrogen pressure or Silicycle or Biotage pre-packed flash columns using Biotage SP1 Flash System using two solvent gradient system. Solvent / Reagent Abbreviations or Formulae used: DCM, Dichloromethane; EtOH, Ethanol; EtOAc, Ethyl acetate; DMSO, Dimethylsulfoxide; MeCN, Acetonitrile; AcOH, Acetic acid; K_2CO_3, Potassium carbonate; KF, Potassium fluoride; Na_2SO_4, Sodium sulfate; KOH, Potassium hydroxide; $FeCl_3$, Ferric chloride; HCl, Hydrochloric acid; Pd/C, Palladium on Carbon. NMR spectra were recorded on either Varian MR 400 MHz, or Varian Inova 500 MHz spectrometer. Chemical shifts were reported in δ (parts per million) in reference to the hydrogen peaks of tetramethylsilane (TMS), δ = 0.00. Mass spectra were recorded on a Micromass LCT Time-of-Flight instrument utilizing electrospray ionization in the positive ion mode (ESI^+).

Synthesis of phenazine derivatives

Scheme 1 represents the overall synthesis procedures of the phenazine compounds. With the previously reported methods (using reagents, a) KF/K_2CO_3 or b) KOH/DMSO),[19] aniline derivatives **1** and 2-fluoronitrobenzene **2** were treated to produce the secondary amine derivatives **3** (N-(4-Aryl)-2-nitroaniline). Using 10% Pd/C catalyst under hydrogen

atmosphere, the nitro group in **3** was reduced to yield the diamine 4 (N-Arylbenzene-1,2-diamine). Then, derivative **4** was oxidised[20] in aqueous ferric chloride solution to produce the corresponding phenazine salts **5** (3-Imino-N,5-bis(aryl)-3,5-dihydrophenazin-2-amine hydrochloride). Following treatments with various primary amines, the phenazine salts **5** yielded the corresponding phenazine derivatives **6** ((E)-3-(Isopropylimino)-N,5-bis(aryl)-3,5-dihydrophenazin-2-amine) with 10 to 85% yield.

Absorbance Measurements

Phenazine derivatives were solubilized at 0.1 mg/ml in methanol and in 9 M H_2SO_4. The UV/Vis spectra of the different phenazine derivatives in methanol and in acidic solutions of H_2SO_4 were obtained in 96 well plates, using a Biotek microplate spectrophotometer.

Physicochemical property predictions

Estimation of various physicochemical properties of clofazimine and its chemical derivatives which could be important for predicting their behaviors when those chemicals are confronted by cellular/suborganellar membranes were made as follows: Clog P (the calculated logarithm of lipid/water partitioning coefficient of nonionic (neutral) forms of the compound) were calculated by Chemaxon software from Marvin Beans (http://www.chemaxon.com/marvin). Clog P values of ionized species were calculated using the procedures described by C. Hansch and A. Leo.[21] Multiple pK_a (the dissociation constant of the protonated functional group) values (pK_{a1}, pK_{a2}, or pK_{a3}) were calculated for the ionizable functional groups (amines) in these weakly basic molecules. Other structure parameters were estimated as described in the next section.[22]

Predicting cellular uptake and intracellular localization of phenazine compounds

Intracellular localization was predicted for each plausible ionic species of each phenazine compound as follow:. For each species, structure parameter values, as estimated above, were inserted into published QSAR models predicting cell uptake and intracellular localizations.[22] The poor-moderate-good predictions in Tables S1, S3 and S5 in the supporting information relate to the log P of the major species present, usually the free base, as follows:

Poor: Clog P>8 or Clog P<0 [and/or number of rotatable bonds >40]; Moderate: 8>Clog P>5; Good: 5>Clog P>0.

Species close to prediction boundaries in parameter space are indicated by use of terms such as moderate-good [i.e., the species falls into the moderate zone, but close to the boundary with the good zone]. Predictions assume that pK_a values of basic groups are such that for most analogues a large proportion of each compound will be present in solution as a free base, with rather less as monocations, and even less as polycations, under physiological conditions. Polycations would only be present within acidic organelles. In Tables S1, S3 and S5: E = endoplasmic reticulum, C = cytosol, G = generic biomembranes, L = lysosome, M = mitochondrion, P = plasma membrane.

Cell culture

Raw 264.7 macrophages or MDCK (Madin Darby Canine Kidney) epithelial cells (strain II) were obtained from American Type Culture Collection (ATCC) (Manassas, VA) and cultured in 75 cm^2 flasks at 37°C, 5% CO_2 containing humidified incubator. RAW 264.7 macrophages (passage numbers 5–15) were grown in the medium containing Dulbecco's Modified Eagle Medium (DMEM (Gibco 11145); Invitrogen, Carlsbad, CA) with 2 mM L-glutamine, 4500 mg/L of D-glucose, 110 mg/L of sodium pyruvate, 1% penicillin-streptomycin (Gibco 10378), and 10% fetal bovine serum (FBS; Gibco 10082). Confluent macrophage cells were detached by scraping and subcultured at 1:8 split ratios to culture flasks. MDCK cells (passage numbers 60–80) were cultured with growth medium consisting of DMEM supplemented with 1× non-essential amino acids (Gibco 11140), 1% penicillin-streptomycin, and 10% fetal bovine serum (FBS). After reaching 70–80% confluence, MDCK cells were detached from the culture flasks using trypsin-EDTA solution, and sub-cultured at a split ratio of 1:5. Media in the flask was replaced every 3 days.

Solubility Measurements

Solutions containing the phenazine derivatives were made in cell culture media (DMEM) with or without FBS (10%). After a 24h incubation, the solutions were centrifuged (10000 × *g*, 10 min), the supernatant was removed and the precipitate was dissolved in 9 M H_2SO_4. The supernatant was diluted with 10 M NaOH to precipitate the remaining solubilized compound. The diluted supernatant was centrifuged (10000 × *g*, 10 min) followed by dissolution of the precipitate in 9 M H_2SO_4. Both fractions were spectrophotometrically measured with a Biotek microplate spectrophotometer (λ=540 nm) and phenazine content was determined using calibrated clofazimine standards.

Cytotoxicity measurements

A XTT colorimetric assay was performed to assess the cytotoxicity of the clofazmine derivatives in Raw 264.7 macrophages or MDCK epithelial cells using a Cell Proliferation Kit II (Roche Chemicals, Indianapolis, IN). Briefly, the cells were seeded in 96 well plates at a cell density of 8×10^3 cells/cm^2 (Raw 264.7 macrophages) or 1.5×10^4 cells/cm^2 (MDCK epithelial cells) and after a 24 h incubation (37°C, 5% CO_2), cells were exposed to media containing various concentrations of clofazmine or its chemical derivatives (100 μL of 0.5, 1, 2, 4, 6, 8, 10, 15, 20, 25, 50 or 100 μM) in DMEM (no phenol red; Gibco 21063) with 5% FBS and 1 mM sodium pyruvate. After 72 h incubation with clofazmine or its derivatives, compound-containing media was removed and cells were washed twice with media. The XTT labeling reagent (3'--bis(4-methoxy-6-nitro)benzene-sulfonic acid hydrate) was freshly mixed with the electron coupling reagent (PMS: N-methyl dibenzopyrazine methyl sulfate) before use according to the manufacturer's instructions. Cells were incubated in 100 μL of media (DMEM with 5 % FBS) with XTT labeling mixture for 3 h (37°C, 5% CO_2). The absorbance value in each well was measured at 495 nm against a reference wavelength at 650 nm using a micro-plate reader (Synergy 2, BioTek Instruments, Winooski, VT). The experiments were repeated in three different sets for the various concentrations of compounds. The IC50 value for each compound was calculated from the concentration-response curve generated by a nonlinear regression (curve fit) method in GraphPad Prism

version 5.0 (GraphPad Software, Inc., San Diego, CA). The concentration of clofazimine or its chemical derivatives used for further *in vitro* cell studies was determined based on cell viability (%) assay results (see the next section).

Cell accumulation experiments and transmitted light microscopic examination

For cell cultures, Raw 264.7 macrophages or MDCK epithelial cells were seeded in the 8-well Nunc™ Lab-Tek™ II chambered (#1.5) coverglasses (Thermo Scientific, Pittsburgh, PA) at a cell density of 8×10^3 cells/cm^2 or 1.5×10^4 cells/cm^2, respectively. After a 24 h incubation (37°C, 5% CO_2), cells were incubated with solution of clofazmine or its chemical derivatives (300 μL of 5 μM concentration; measured cell viability ranging from 85 to 97% for all compounds tested at this concentration; Figure 1) in DMEM (no phenol red; plus 1 mM sodium pyruvate and 5% FBS). For compound "I", 2.5 μM of compound solution in media was used for the Raw 264.7 macrophages incubation because of lower cell viability at higher concentrations (IC50 = 3.95 ± 0.11 μM). A solution of clofazmine or other chemical derivatives was made by a diluting stock solutions (2.5 mM in DMSO; 10 mM stock in DMSO were stored at −80°C for further use) into DMEM with 5% FBS. Previously, we reported that clofazmine did not form visible precipitates in this media (DMEM with 5% FBS).[7] For other phenazine derivatives, precipitates were avoided by including FBS in the media. The extracellular concentration of each compound in each well was maintained by daily replacement of the compound-containing media. After 72 h of incubation with clofazmine or its derivatives, compound-containing media were removed and cells were washed twice with media. Live cells in the chambered glasses were examined under inverted transmitted light microscopy (Nikon Eclipse T*i* microscope) with a 40 × objective and color camera. As a control experiment, fixed Raw 264.7 macrophages or MDCK epithelial cells were also microscopically examined after incubation with the compounds. Cells were seeded on the chambered cover glasses at the density of 1.5×10^4 cells/cm^2 (RAW264.7 macrophages) or 2.5×10^4 cells/cm^2 (MDCK epithelial cells). After an overnight incubation (37°C, 5% CO_2), media was removed from the wells and cold methanol (−20°C) was added to each well. After 30 sec, remaining methanol was removed by washing with media with 5% FBS. Fixed cells were incubated (37°C, 5% CO_2) with clofazmine or derivatives (300 μL of 5 μM; 2.5 μM for I) in media with 5% FBS. After 72 h, fixed 264.7 or MDCK cells were washed with media and examined using the same transmitted microscopy conditions as the live cells.

Cell associated mass measurements

Raw 264.7 macrophages or MDCK epithelial cells were seeded in 96 well plates at the density of 8×10^3 cells/cm^2 or 1.5×10^4 cells/cm^2, respectively. After an overnight incubation (37°C, 5% CO_2), cells were incubated with 100 μL of the media (DMEM with 5% FBS) containing 5 μM clofazmine or its chemical derivatives (2.5 μM of compound "I"). Media containing each compound was replaced every day during the 72 h incubation. After the incubation, media was removed and cells were washed with HBSS buffer (No.14025; Invitrogen) twice. RAW 264.7 macrophage cells in buffer were scraped and MDCK epithelial cells were exposed to Trypsin-EDTA solution for detachment from the plates for cell number counting and quantification of cell-associated masses. After centrifugation (650 × *g*), supernatant was removed and cell pellets were resuspended in 0.1 M citric acid/0.1M

trisodium citrate buffer (pH 5) for cell counting as previously reported.[7] Equal numbers of cells in 100 μL in buffer were transferred to 96 well plates and 100 μL of detergent (ATCC, 30–1010K™) was added into wells for cell lysis. Chemical absorbance from each well was measured by the UV/Vis micro-plate reader (Synergy 2, BioTek Instruments, Winooski, VT) at 490 nm wavelength and cell-associated mass of each compound was calculated by a standard curve generated separately using the same media, and presented as pmole/cell by normalizing the amount of chemical in each cell population sample by the number of cells in each sample.

Linear diattenuation microscopy instrument set up

The LC-PolScope was first developed as a birefringence imaging system at the Marine Biological Laboratory (Woods Hole, MA) by R. Oldenbourg and colleagues, which greatly increased the sensitivity and analytic power of the polarized light microscope.[9] Recently, the technique was extended to include quantitative imaging of diattenuation and polarized fluorescence in biological and man-made specimens.[10, 23] For our studies of absorption properties of intracellular aggregates of phenazine derivatives, we used the diattenuaton LC-PolScope as reported earlier[10] and described on the website OpenPolScope.org. The optical design was built on a Nikon Eclipse T*i* microscope equipped with the liquid crystal universal compensator consisting of a linear polarizer and a pair of liquid crystal devices. The LC compensator was part of the trans-illumination path and was used to illuminate the specimen with monochromatic, linearly polarized light of varying polarization orientation. There was no polarization analyzer present in the imaging path. Quantitative intensity images were recorded by a charge-coupled device (CCD) camera and a desktop computer calculated the average transmittance, the differential transmittance and the polarization orientation leading to maximum transmittance for each optically resolved picture element (pixel). Acquisition and processing steps were controlled using OpenPolScope plugins for the open source imaging programs ImageJ and Micro-Manager (MMStudio version 1.4.15). With the combination of hardware and software, polarized light images were acquired at high sensitivity and high spatial resolution for measuring linear diattenuation.

Linear diattenuation microscopy data acquisition and analysis

After RAW264.7 macrophages or MDCK epithelial cells were incubated with the compound in the chambered cover glasses for 72 h, at the same time of performing transmitted microscopic examination, cell specimens were examined under linear diattenuation microscopy using the Nikon Eclipse T*i* microscope with 40×/0.75 NA objective and monochromatic light of two different center wavelengths, 546 and 623 nm (passband 30 nm). In the OpenPolScope software, Pol-Acquisition and Pol-Analyzer plugins (version 2.0) were used to capture, process, and analyze the attenuation images. Before imaging the samples, the setup was calibrated using a specially prepared slide featuring 4 small pieces of linear polarization filters. The transmission axes of the filters were oriented in steps of 45° providing a means to calibrate the LC universal compensator settings. After the calibration, a sample slide was inserted and first a sequence of polarized light images of a clear, fully transmitting sample area was recorded, followed by an image sequence featuring the cells under investigation. The images of the clear area were used to determine instrument factors

which were needed for computing the average and the polarization dependent loss in transmittance in cellular components visible in the second image [10].

Linear diattenuation is a material property that can occur in materials such as crystals, in which the light absorbing molecules are arranged with a preferred orientation. The molecular alignment creates principal axes in the material denoting polarization directions for which light is maximally and minimally transmitted. Diattenuation is the difference between maximal (T_{max}) and minimal (T_{min}) transmittance, divided by their sum (Equation 1):

$$Diattenuation = \frac{T_{\max} - T_{\min}}{T_{\max} + T_{\min}} \quad (1)$$

To simultaneously measure the attenuation of many crystals with arbitrary orientations, we developed algorithms based on 4 specimen images, each recorded using light of a different polarization orientation: 0°, 45°, 90°, and 135°.[10] The 4 raw images were used to calculate the average and differential transmittance, and the orientation of maximum transmittance in every resolved image pixel. To isolate and analyze quantitative data of the objects (crystals), the anisotropy or maximum transmittance axis orientation image file opened in ImageJ was inverted (Ctrl+Shift+I) and thresholded using ImageJ's default automatic method ("Binary" → "Convert to Mask"). By using the ImageJ's algorithm, "Analyze Particles", data of anisotropy or maximum transmittance axis orientation of objects in images could be obtained automatically. Diattenuation ratios were calculated by dividing anisotropy at 623 nm by that at 546 nm. For images obtained from cells incubated with compounds, P, U, V, or W, maximum transmittance axis orientation lines in crystals were displayed by using OpenPolScope's plugin (Orientation-LinesV3) installed in ImageJ.

Confocal fluorescent microscopy

A Nikon A1 confocal microscope was used for further investigation of live cells incubated with chiral pairs of compounds (T and U) and the parent compound, P. Since crystals or vesicular forms containing chemicals inside the cells incubated with compound P, T, or U were fluorescent when viewed with the TRITC filter sets, intracellular distribution of these compounds in 264.7 or MDCK cells were visualized using a Nikon A1 confocal microscopy (Nikon Instruments Inc., Melville, NY) equipped with diode-based lasers and a Nikon Apo 60× /1.4 NA oil immersion lens. Briefly, RAW264.7 macrophages or MDCK epithelial cells were seeded in the 8-well Nunc™ Lab-Tek™ II chambered (#1.5) cover glasses (Thermo Scientific, Pittsburgh, PA) at a density of 8×10^3 cells/cm^2 (264.7 cells) or 1.5×10^4 cells/cm^2 (MDCK cells) and allowed to adhere overnight (37°C, 5% CO_2). Then, 5 μM of compound 'P' or the related isomers, 'T' or 'U' in DMEM with 5% FBS (300 μL) was added to the cells and the cells were incubated for 72 h (37°C, 5% CO_2). For live cell imaging, after the removal of media, cells were washed with HBSS buffer twice. Hoechst 33342 (Invitrogen, Carlsbad, CA) was used for staining cell nuclei and FM® 1–43 (Molecular Probes T35356, Invitrogen) for the plasma membrane. Cells were incubated with 300 μL of 1:1 (v/v) dye mixtures of 5 μg/ml Hoechst 33342 and 7 μM FM® 1–43 in HBSS for 15 min at room temperature. Without fixative, the confocal imaging of the live cells was

performed using lasers for DAPI (excitation/emission wavelength: 405 nm/450 ± 25 nm), FITC (488 nm/525 ± 25 nm), and TRITC (561 nm/596 ± 25 nm) channels. Z-stack images of the cells were captured along the Z-axis (interval, 1 μm) in three fluorescence channels and analyzed by using the Nikon NIS-Elements 3.2 confocal software (Nikon Instruments Inc., Melville, NY). In three dimensional reconstructions of the confocal sections assembled with the Nikon software, the cell nuclei fluoresced in the Hoechst/DAPI channel; the cell membranes fluoresced in the FITC channel; and, the intracellular inclusions fluoresced in the TRITC channel.

Transmittance and optical density calculations

For calculating the differential transmittance of the inclusions, images at 4 different angles of polarization (0°, 45°, 90°, and 135°) were acquired by linear attenuation microscopy as described above. To measure transmittance, a threshold was applied to the mean transmitted image generated by the linear attenuation microscopy data acquisition. This threshold was determined using the ImageJ Auto-thresholding protocol – Moments. Based on this threshold, a region of interest (ROI) image mask was generated, and then used to measure the mean transmittance (T_{mean}) of the ROIs, expressed as mean pixel value. To generate transmittance image maps and for quantitative measurement of transmittance, pixel values were converted to absolute values by dividing the mean pixel value by 255 (8-bit images). For the corresponding optical density (OD) image maps and measurements, we used the following formula: $OD = -\log_{10}(T_{mean})$. For each compound a total of five images were measured from experiments performed on three separate days (>200 cells analyzed per compound).

Principal component analysis (PCA)—An “optical properties score” was calculated for each replicate measurement (n=5) for each compound in each cell type (Raw 264.7 macrophages and MDCK epithelial cells), by combining the anisotropy and optical density values at 546 and 623nm wavelengths. PCA plots[24] were generated using SIMCA (the standard in multivariate data analysis) software (http://www.umetrics.com/products/simca; Umeâ, Sweden).

Supplementary Material

Refer to Web version on PubMed Central for supplementary material.

Acknowledgements

We acknowledge financial support from NIH (grant R01GM078200 to G.R.R; R01EB002583 to R.O.); a Rackham Predoctoral Fellowship Award to KAM; and, University of Michigan M-Cubed funds awarded to KAS and GRR; RWH thanks Dr. R. Aitken, School of Life Sciences, University of Glasgow for provision of facilities.

References

1. a) Serbina NV, Jia T, Hohl TM, Pamer EG. Annu. Rev. Immunol. 2008; 26:421–452. [PubMed: 18303997] b) Mantovani B, Rabinovitch M, Nussenzweig V. J Exp. Med. 1972; 135:780–792. [PubMed: 5018051] c) Ricardo SD, van Goor H, Eddy AA. J Clin. Invest. 2008; 118:3522–3530. [PubMed: 18982158] d) Murray PJ, Wynn TA. Nat. Rev. Immunol. 2011; 11:723–737. [PubMed: 21997792]

2. a) Conalty ML, Barry VC, Jina A. Int. J. Lepr. Other Mycobact. Dis. 1971; 39:479–492. [PubMed: 4948088] b) Reasor MJ. Res. Commun. Chem. Pathol. Pharmacol. 1991; 72:169–181. [PubMed: 1876748] c) Brown MS, Goldstein JL. Annu. Rev. Biochem. 1983; 52:223–261. [PubMed: 6311077] d) Anderson N, Borlak J. FEBS Lett. 2006; 580:5533–5540. [PubMed: 16979167]
3. a) Atkinson AJ Jr, Sheagren JN, Rubio JB, Knight V. Int. J. Lepr. Other Mycobact. Dis. 1967; 35:119–127. [PubMed: 5338956] b) http://www.who.int/medicines/publications/essentialmedicines/en/.
4. a) Baik J, Rosania GR. PLoS One. 2012; 7:e47494. [PubMed: 23071814] b) Baik J, Stringer KA, Mane G, Rosania GR. Antimicrob. Agents Chemother. 2013; 57:1218–1230. [PubMed: 23263006]
5. Kaufmann AM, Krise JP. J Pharm. Sci. 2007; 96:729–746. [PubMed: 17117426]
6. Horobin RW, Trapp S, Weissig V. J Control. Release. 2007; 121:125–136. [PubMed: 17658192]
7. Baik J, Rosania GR. Mol. Pharm. 2011; 8:1742–1749. [PubMed: 21800872]
8. a) Fahr A, van Hoogevest P, Kuntsche J, Leigh ML. J Liposome Res. 2006; 16:281–301. [PubMed: 16952882] b) Fahr A, van Hoogevest P, May S, Bergstrand N, ML SL. Eur J Pharm Sci. 2005; 26:251–265. [PubMed: 16112849]
9. a) Oldenbourg R. Nature. 1996; 381:811–812. [PubMed: 8657288] b) Oldenbourg R, Mei G. J Microsc. 1995; 180:140–147. [PubMed: 8537959] c) Shribak M, Oldenbourg R. Appl. Opt. 2003; 42:3009–3017. [PubMed: 12790452]
10. Mehta SB, Shribak M, Oldenbourg R. J Opt. 2013; 15:094007–094020.
11. Beis I, Newsholme EA. Biochem. J. 1975; 152:23–32. [PubMed: 1212224]
12. Hwang C, Sinskey AJ, Lodish HF. Science. 1992; 257:1496–1502. [PubMed: 1523409]
13. a) Lodish, H. Molecular cell biology. New York: W.H. Freeman and Company; 2008. b) Cooper, GM.; Hausman, RE. The cell: A molecular approach. Sunderland: Sinauer Associates; 2000.
14. a) Gottfried EL. J Lipid Res. 1967; 8:321–327. [PubMed: 5231291] b) Machaiah J, Vakil U. J Biosci. 1989; 14:367–377.
15. Fu D, Zhou J, Zhu WS, Manley PW, Wang YK, Hood T, Wylie A, Xie XS. Nat. Chem. 2014; 6:614–622. [PubMed: 24950332]
16. Boland MV, Murphy RF. Bioinformatics. 2001; 17:1213–1223. [PubMed: 11751230]
17. a) Rin Jean S, Tulumello DV, Wisnovsky SP, Lei EK, Pereira MP, Kelley SO. ACS Chem. Biol. 2014; 9:323–333. [PubMed: 24410267] b) Mourtada R, Fonseca SB, Wisnovsky SP, Pereira MP, Wang X, Hurren R, Parfitt J, Larsen L, Smith RA, Murphy MP, Schimmer AD, Kelley SO. PLoS One. 2013; 8:e60253. [PubMed: 23585833]
18. Vendrell M, Lee JS, Chang YT. Curr. Opin. Chem. Biol. 2010; 14:383–389. [PubMed: 20227904]
19. a) Xu Z-B, Lu Y, Guo Z-R. Synlett. 2003; 4:564–566.b) Kirsch P, Schonleben-Janas A, Schirmer RH. Liebigs Annalen. 1995; 1995:1275–1281.
20. a) O'Sullivan JF, Conalty ML, Morrison NE. J Med. Chem. 1988; 31:567–572. [PubMed: 3279207] b) O'Sullivan JF. J Chem. Res., Miniprint. 1984; 52
21. Hansch, C.; Leo, A. New York: Wiley; 1979. p. 18-43.
22. a) Horobin RW, Rashid-Doubell F, Pediani JD, Milligan G. Biotech. Histochem. 2013; 88:440–460. [PubMed: 23758207] b) Horobin RW, Rashid-Doubell F. Biotech. Histochem. 2013; 88:461–476. [PubMed: 23758208]
23. DeMay BS, Noda N, Gladfelter AS, Oldenbourg R. Biophys. J. 2011; 101:985–994. [PubMed: 21843491]
24. Abdi H, Williams LJ. Wiley Interdisciplinary Reviews: Computational Statistics. 2010; 2:433–459.

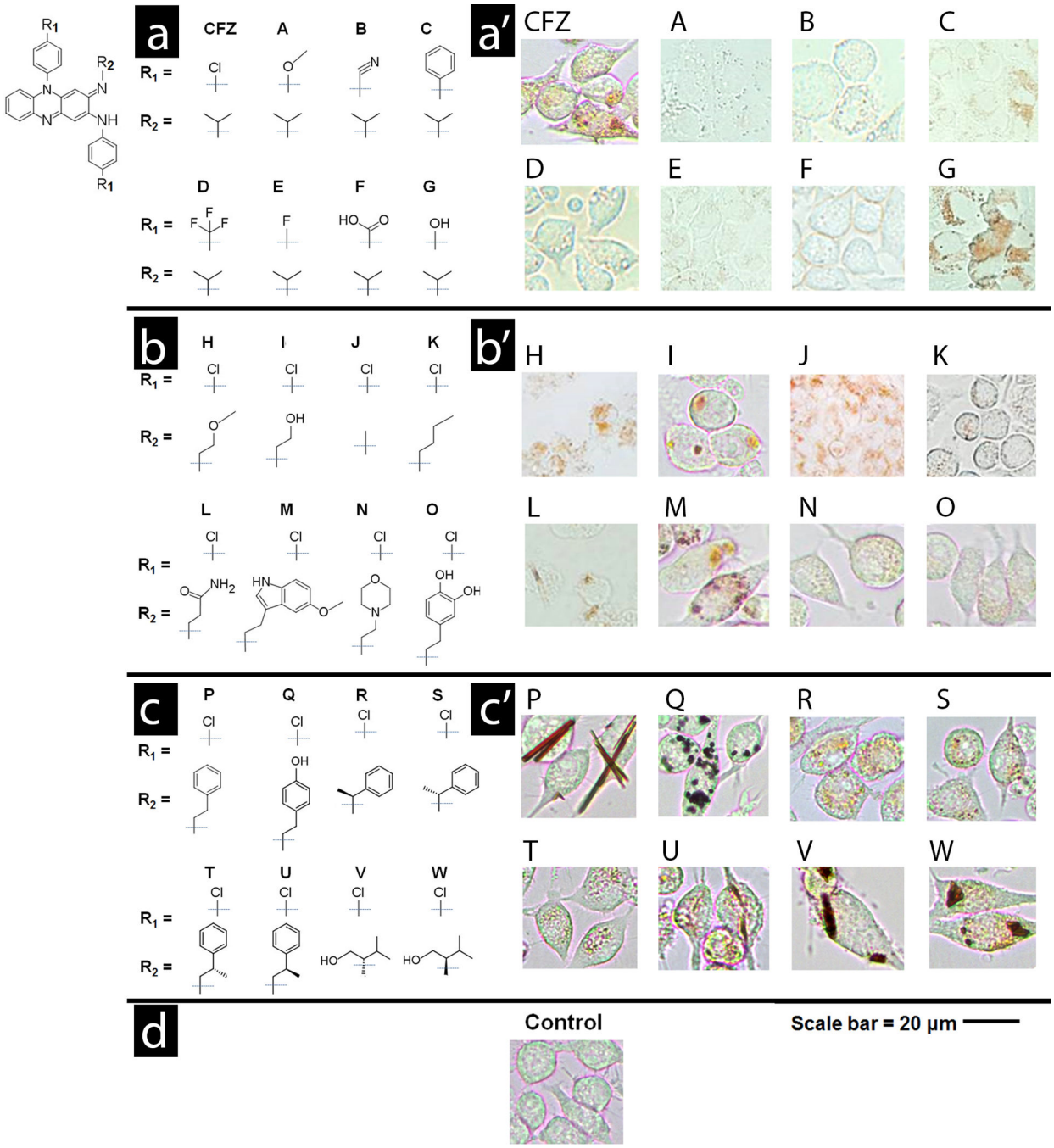

Figure 1.

Three series of phenazine derivatives of clofazimine were synthesized to probe the relationship between clofazimine's chemical structure (a, b and c) and its cellular staining patterns (a', b' and c'). The common phenazine core shared by all phenazine compounds is shown in the top left corner of the figure. In the first series of derivatives (a and a'), the chlorophenyl groups of clofazimine were substituted with different functionalities. In the second series (b and b'), the isopropyl R-imino group of clofazimine was substituted with achiral functional groups. In the third series (c and c') the isopropyl R-imino group of

clofazimine was substituted with additional functional groups that probed the effects of an added stereochemical center. Scale bar = 20 μm.

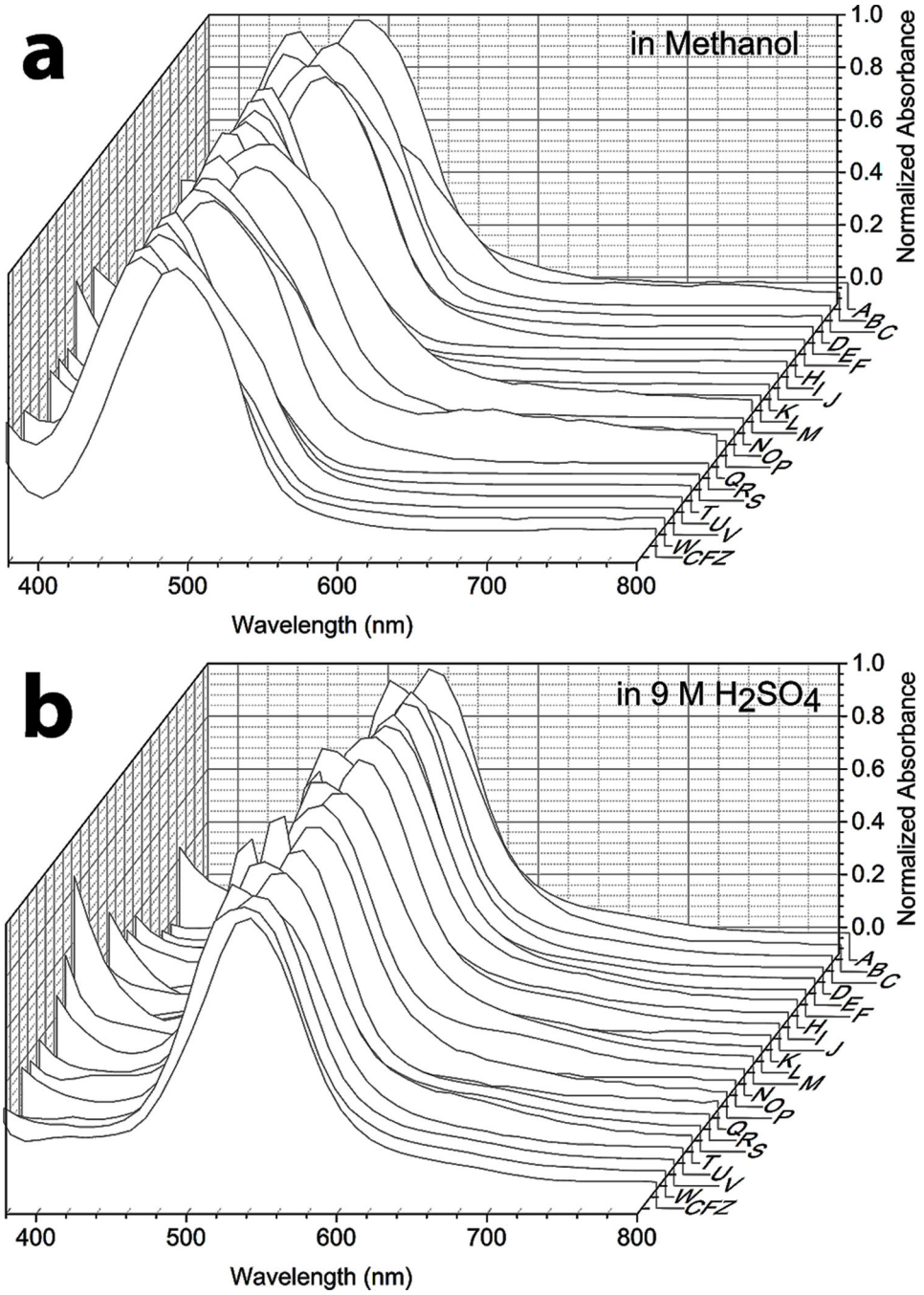

Figure 2.

Absorbance spectra of phenazine compounds were very similar to that of clofazimine. Absorption peaks were between 450 and 490 nm when measured in methanol and between 510 and 540 nm when measured in H_2SO_4.

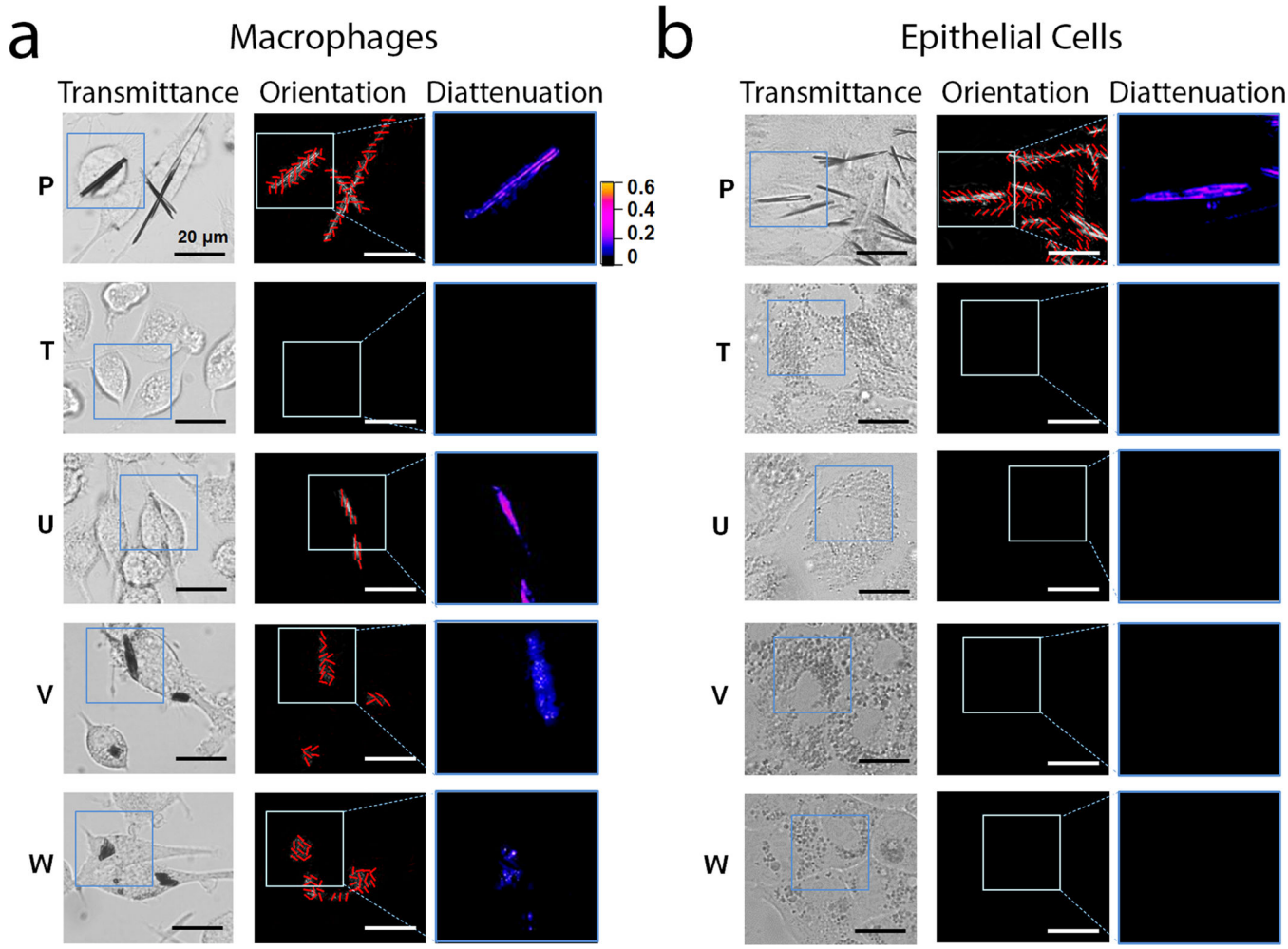

Figure 3.

Quantitative polarization microscopy of macrophages and epithelial cells incubated with the different phenazine compounds revealed cell type-specific differences in transmittance, diattenuation anisotropy, and the orientation of the polarization axis maximal transmittance of the intracellular inclusions. For the experiments, live RAW264.7 macrophages (a) or MDCK epithelial cells (b) were incubated for 72 hours with clofazimine or other phenazine analogs, and analyzed with the diattenuation anisotropy microscope imaging set up, using monochromatic light of 546 nm wavelength. Transmittance corresponds to the image map of the transmitted light intensity at 546 nm wavelength (white corresponds to 100% transmittance and black corresponds to 0% transmittance); Orientation corresponds to the measured direction of maximal light transmittance of linearly polarized light across the sample, indicated with a grid of red lines superimposed on the image. Diattenuation corresponds to the quantitative diattenuation anisotropy image map measured using linearly polarized light of 546 nm wavelength. The color-gradient calibration bar corresponds to diattenuation anisotropy values ranging from 0 to 0.6. Scale bar = 20 μm.

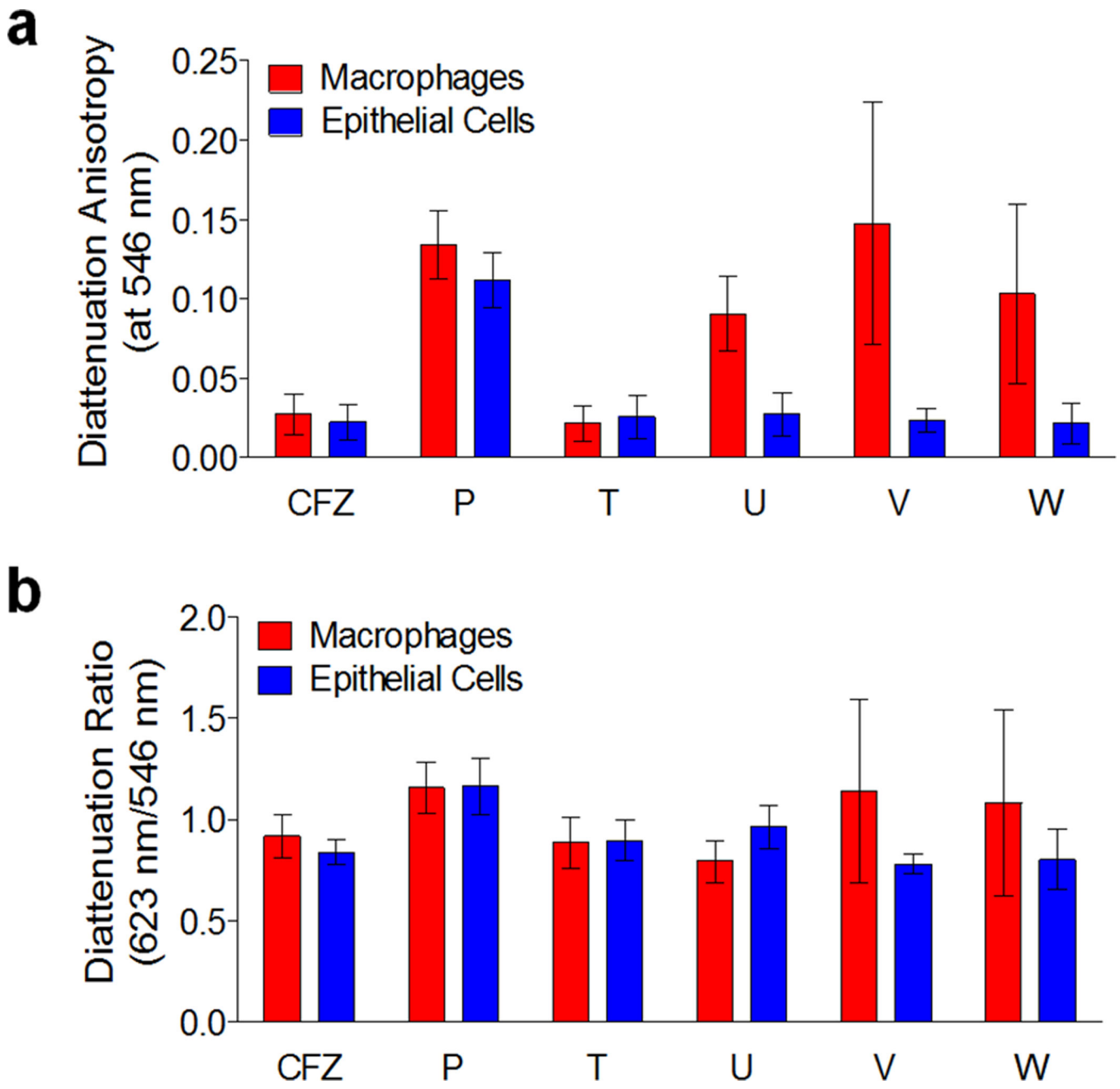

Figure 4.

Quantitative comparison of the diattenuation anisotropy measurements of intracellular inclusions formed by clofazimine and other phenazine derivatives showing the most prominent diattenuation anisotropy signals (Componds P, U, V and W). Compound T was included as well, since it corresponds to the mirror image (chiral pair) of Compound U. a) Compared to clofazimine, compounds U, V and W show stronger diattenuation anisotropy signals in macrophages, while Compound P shows stronger diattenuation anisotropy signals in both macrophages and epithelial cells. b) The ratio of 623 nm / 546 nm diattenuation anisotropy signals of the phenazine compounds were similar to that of clofazimine.

Suggesting greater variability in the organization of the intracellular inclusions, Compounds V and W exhibited greater standard deviations, corresponding to greater differences in the measured diattenuation anisotropy ratios amongst individual inclusions.

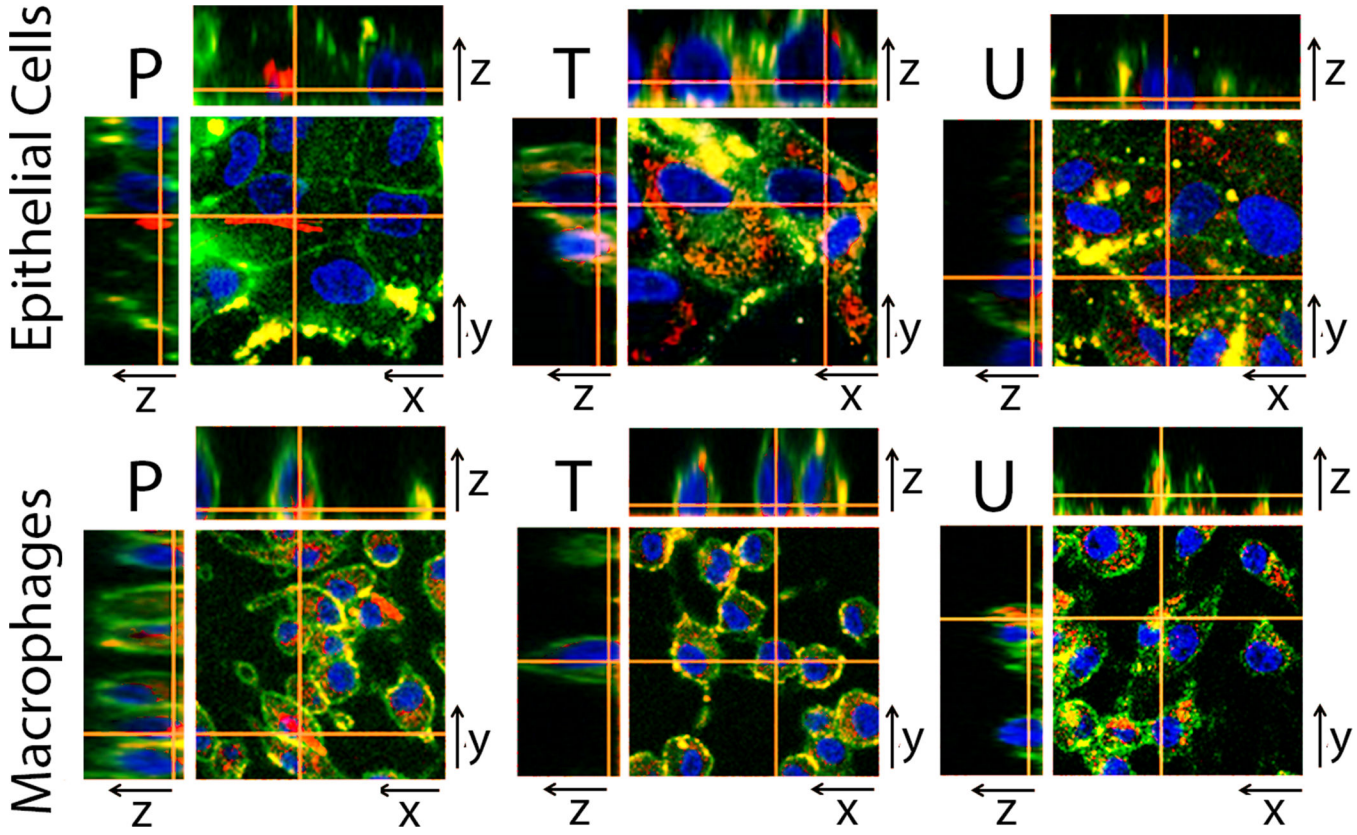

Figure 5.

Confocal fluorescence microscopy of Raw 264.7 macrophages or MDCK epithelial cells after incubation with fluorescent phenazine compounds, P, T, or U. Two dimensional images in xy planes show the location of cell nuclei (blue) and plasma membranes (green), together with the corresponding, intracellular location of phenazine compounds (red). Three dimensional reconstructions of optical sections through orthogonal planes (xz and yz planes) confirm intracellular, cytoplasmic signals of compounds (red), in relation to the position of the nuclei and plasma membrane signals. Scale bar = 20 μm.

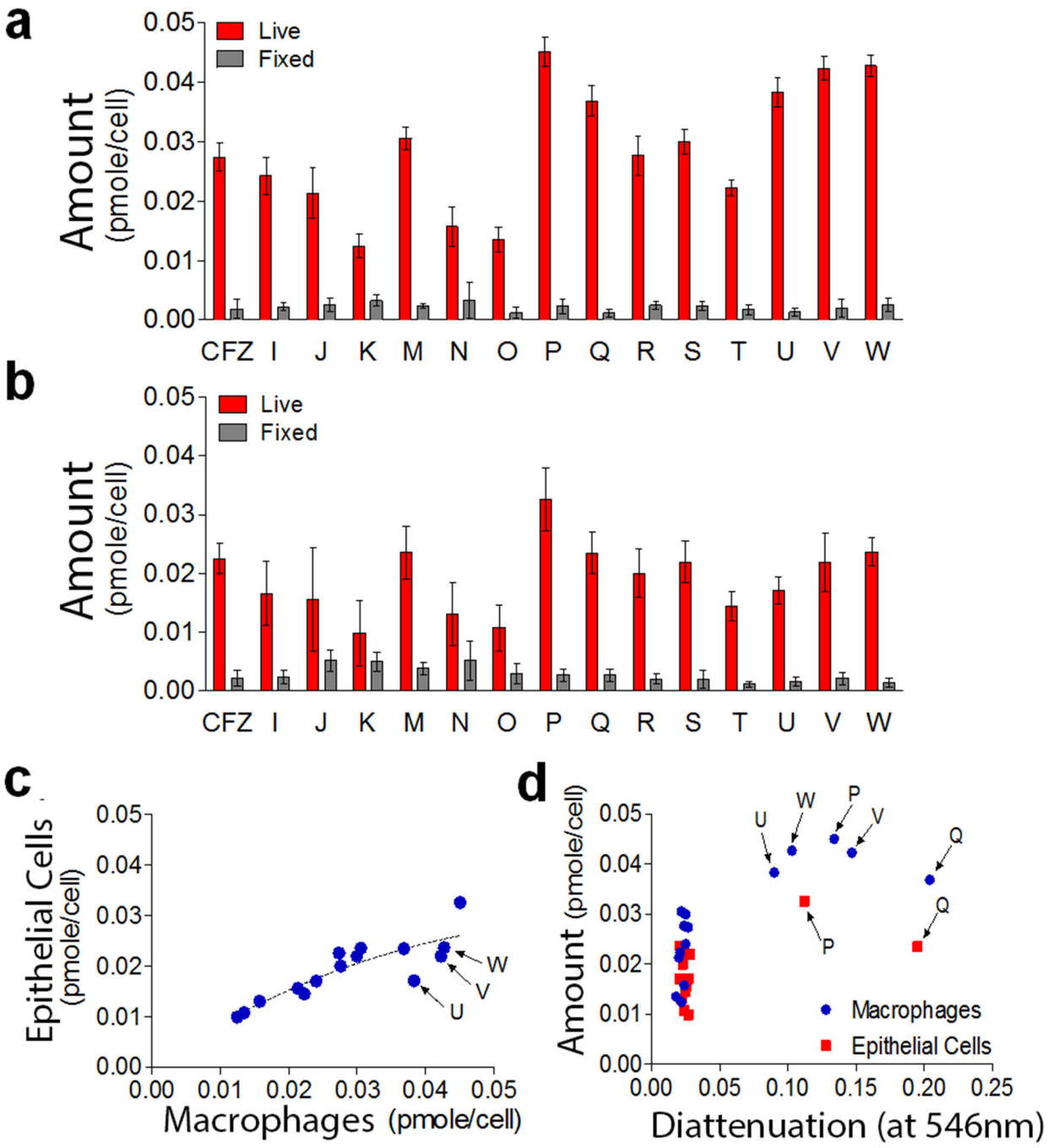

Figure 6.

Measured differences in the accumulation of clofazimine or its phenazine derivatives (in pmols per cell) in Raw 264.7 macrophages or MDCK epithelial cells following a 72 hour incubation period. a) Measurements indicate significant differences in the accumulation of the compounds in live vs. fixed macrophages. b) Measurements also indicate significant differences in the accumulation of the compounds in live vs. fixed epithelial cells. (c) Plot of mass accumulation of compounds in macrophages vs. epithelial cells reveals overall trend towards higher accumulation of the compounds in macrophages. (d) Plot of the cellular

accumulation of phenazine compounds in macrophages and epithelial cells in relation to the diattenuation anisotropy of the resulting intracellular inclusions, measured using linearly polarized light at 546 nm wavelength.

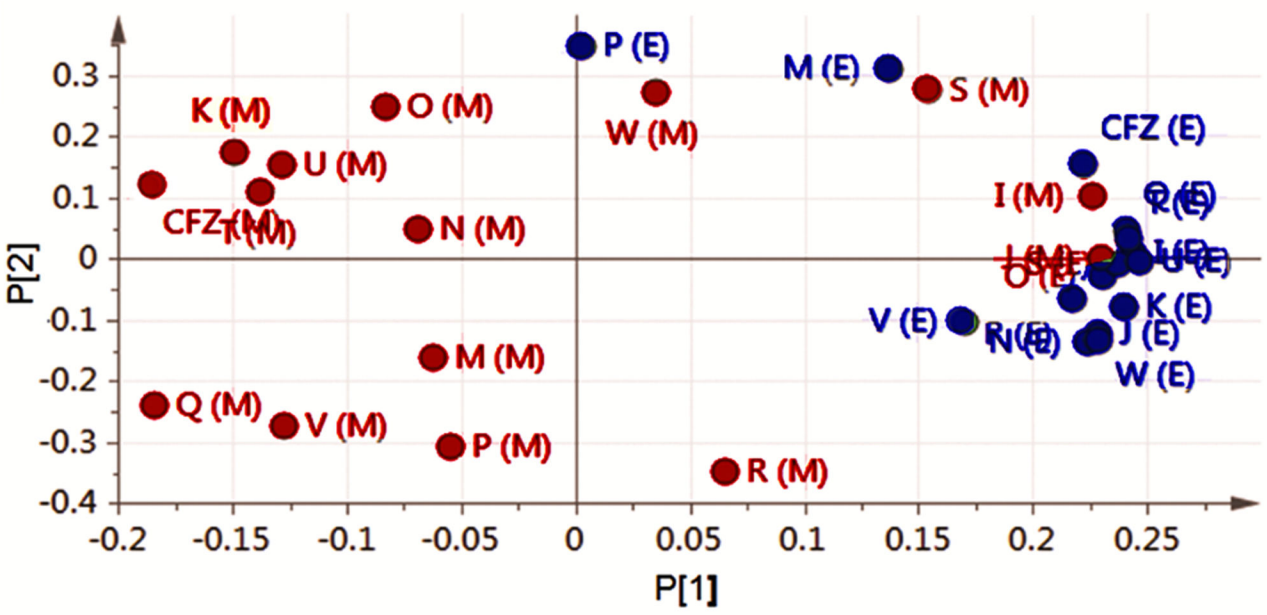

Figure 7.

Principal component analysis (PCA) confirms that the cell-associated staining patterns of phenazine compounds corresponded with a greater variation in bioaccumulation and optical signals in macrophages. PCA was performed based on all optical properties analyzed for each phenazine compound in series 2 and 3, using five replicate measurements at 546 and 623 nm. In the plot, X(M) corresponds to compound X in macrophages (red) and X(E) corresponds to compound X in epithelial cells (blue). In this PCA plot, only the two main principal components are shown. These first two components of the PCA plot explained 97% of the variance in the data.

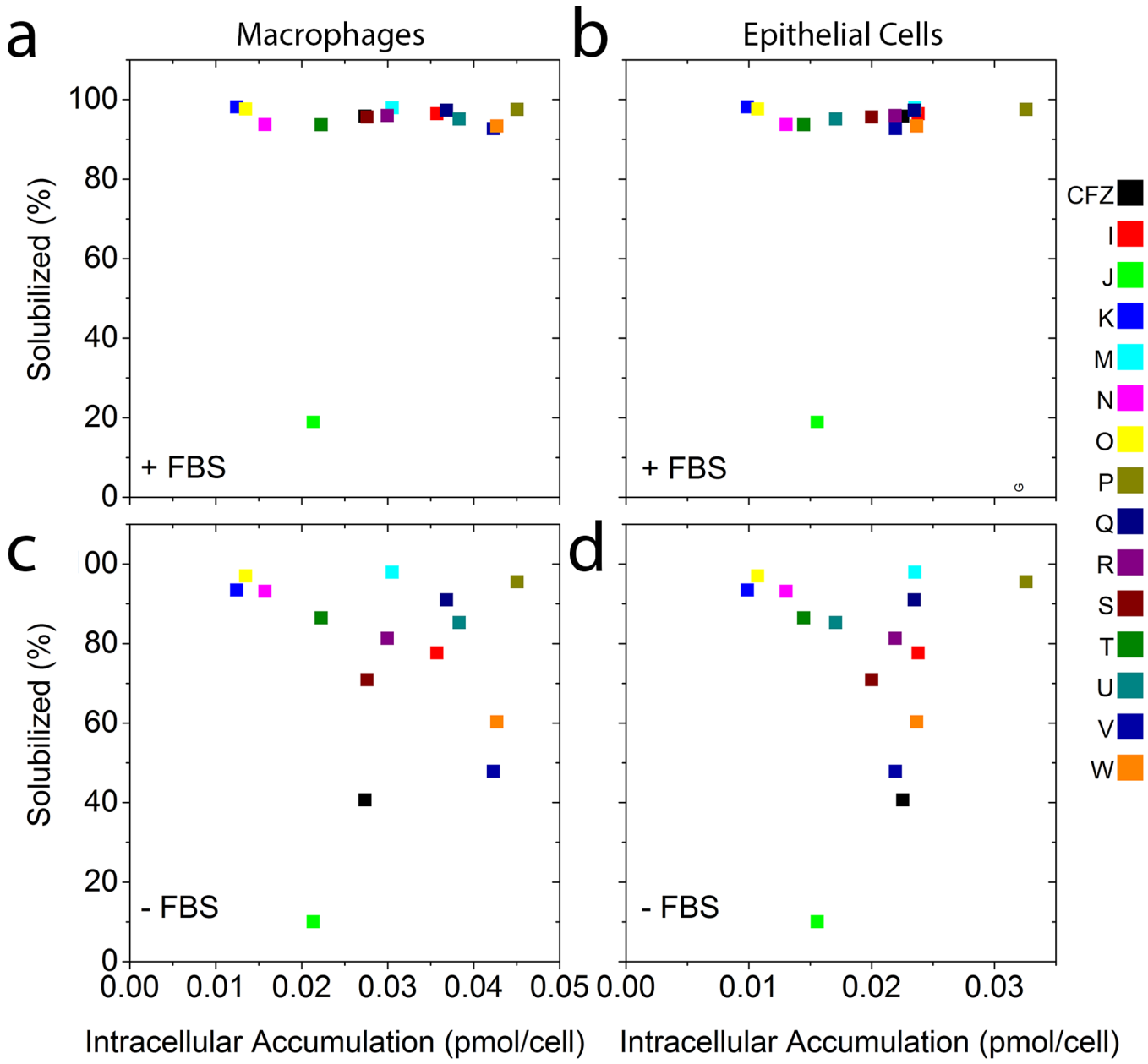

Figure 8.

The solubility of phenazine compounds in cell culture media with (+FBS; a and b) and without fetal bovine serum (−FBS; c and d) plotted in relation to their cellular accumulation in RAW264.7 macrophages (a and c) and MDCK epithelial cells (b and d).

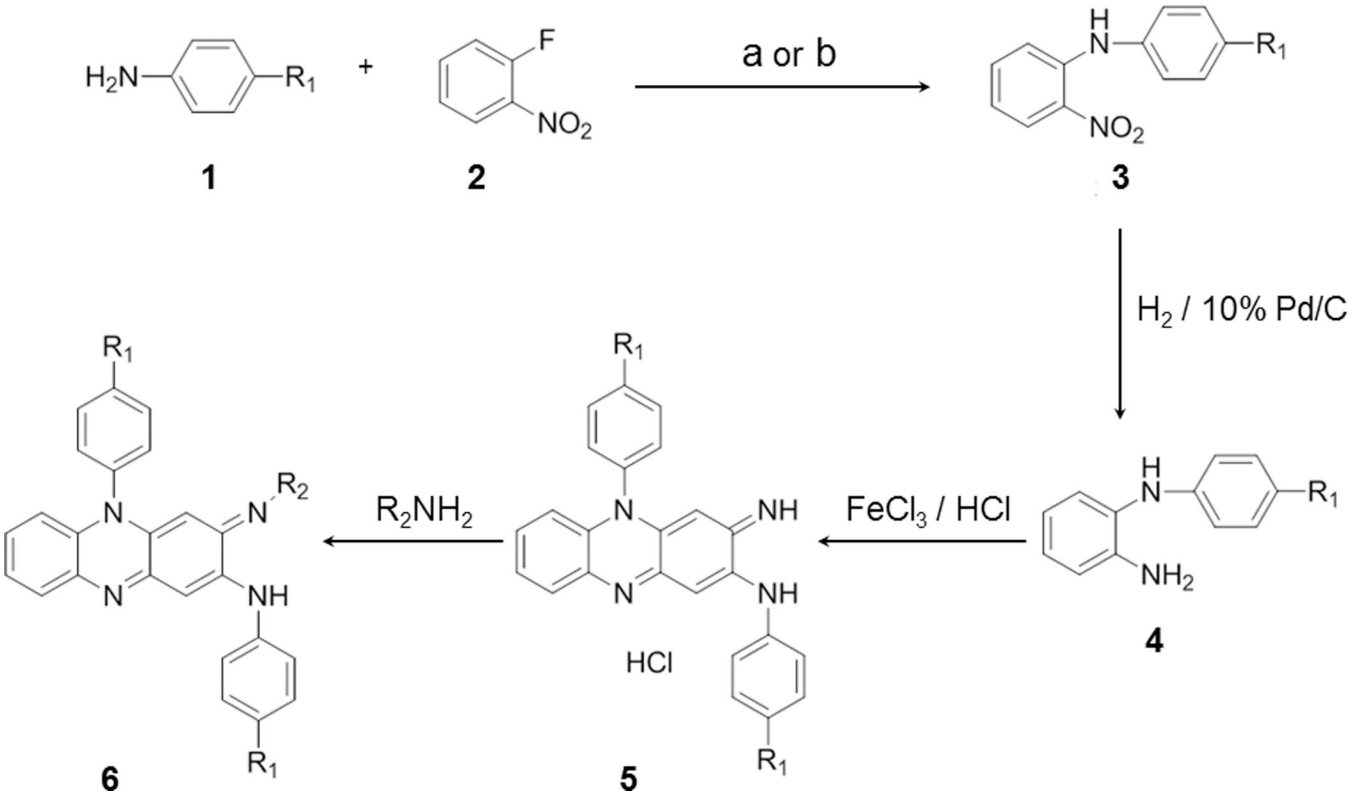

Scheme 1.

Synthesis of phenazine derivatives. Treatment of aniline derivatives **1** with 2-fluoronitrobenzene **2** (using reagents a) KF/K_2CO_3 or b) KOH/DMSO) gave the secondary amine derivatives **3** in 22 to 63% yield. Reduction of the nitro group was carried out using 10% Pd/C catalyst under hydrogen atmosphere to yield the diamine **4** in 55 to 99% yield. Then the diamine **4** was oxidised in aqueous ferric chloride solution to give the corresponding phenazine salts **5** in 70 to 96% yield. The phenazine salts **5** on treatment with variety of primary amines gave the corresponding phenazine derivatives **6** in 10 to 85% yield. These methods are elaborated in detail in the Supplementary Materials.